Showcasing collaborative research from the R. A. Fischer and R. Gläser labs at Ruhr-University Bochum, Technical University Munich and University of Leipzig.

Simultaneous introduction of various palladium active sites into MOF *via* one-pot synthesis: Pd@$[Cu_{3-x}Pd_x(BTC)_2]_n$

Simultaneous incorporation of Pd^{2+}/M^{2+}-nodes and Pd^0 nanoparticles dispersion into MOF are achieved *via* one-pot synthesis. The Pd^{2+}-sites in such designed solids play an important role in enhancing the catalytic activity on the hydrogenation of *p*-nitrophenol with $NaBH_4$ to *p*-aminophenol.

ROYAL SOCIETY OF CHEMISTRY

www.rsc.org/dalton

Simultaneous introduction of various palladium active sites into MOF *via* one-pot synthesis: Pd@[Cu₃₋ₓPdₓ(BTC)₂]ₙ†

Wenhua Zhang,[a] Zhihao Chen,[b] Majd Al-Naji,[b] Penghu Guo,[c] Stefan Cwik,[a] Olesia Halbherr,[a] Yuemin Wang,[d] Martin Muhler,[c] Nicole Wilde,[b] Roger Gläser[b] and Roland A. Fischer*[e,f]

Simultaneous incorporation of palladium within Pd–Pd and/or Pd–Cu paddlewheels as framework-nodes and Pd nanoparticle (NP) dispersion into MOF have been achieved for the first time *via* one-pot synthesis. In particular, the framework substitution of Cu^{2+} by Pd^{2+} as well as the pore loading with PdNPs have been confirmed and characterized by XPS. The obtained solids featuring such multiple Pd-sites show enhanced catalytic activity in the aqueous-phase hydrogenation of *p*-nitrophenol (PNP) with NaBH$_4$ to *p*-aminophenol (PAP).

High structural and compositional design ability of metal–organic frameworks (MOFs) and hence, the ability of tailoring their properties made MOFs to be among the most topical materials over last decades.[1–7] Along with linker(s) modification[8–10] and guest(s) inclusion,[11,12] variation of the metal center(s) is also a powerful tool to fine tune MOFs functionalities. In fact, both control over coordinatively unsaturated metal sites (CUS) (*e.g.*, *via* "defects-engineering")[13] and partial metal substitution (*e.g.*, *via* "solid solution" approach) could considerably enhance MOFs activity, particularly in catalysis[14–16] and selective gas sorption/separation.[17,18]

Combination of distinct metal-ions, which are closely related in coordination chemistry and have similar effective ionic radii (r_{ion}), such as Cu^{2+} (73 pm)/Zn^{2+} (74 pm) couple[19]

within single MOF, has been reported for several structural types.[17,20,21] In fact, partial substitution of Cu^{2+} by Zn^{2+} and some other metals of 3d-row, namely, Co, Fe and Mn, in HKUST-1 ([Cu$_3$(BTC)$_2$]$_n$, BTC = benzene-1,3,5-tricarboxylate) has been recently reported.[18,22] In a later case, doping with a second metal caused enhanced selective sorption of O$_2$ *vs.* N$_2$.[18,23] What is more challenging, however, is to introduce more distinct metals of 4d-[24] or 5d-row[25] as framework-nodes. In particular, metals of the platinum group are highly attractive as catalytic/strong sorption centers. Moreover, square planar coordination is preferred such as Cu^{2+}.[26–28,29] However, due to kinetic reasons, these metal ions are difficult to be crystallized within 3D structures[28,29] and therefore, are almost neglected in MOF field.[30] To the best of our knowledge, studies on integration of palladium as a framework node into a MOF are thus far in its infancy.[30–33] Reports on MOFs featuring Pd–Pd and Pd–M paddlewheel nodes could not be found. Interestingly, bimetallic Pd/M-paddlewheel complexes have been lately found to be promising economical catalysts in the intramolecular benzylic C–H amination.[34] Moreover, porous metal–organic polyhedrals (MOPs) constructed with Pd^{2+}–M^{2+} (M = Cu, Ni, Zn) paddlewheel nodes has been very recently described.[29] Considering its structural peculiarities (*i.e.*, paddlewheel SBUs and CUSs), choosing HKUST-1 as a matrix for palladium in-framework incorporation *via* solid solution approach would be of interest.[35] However, a rigorous exclusion of reducing conditions during MOF synthesis is difficult. Even technical activation may cause reduction at some metal sites due to decarboxylation.[36,37] Therefore, the standard protocol for HKUST-1 synthesis is, intentionally, not changed at this stage.

On the other hand, loading of Pd^0 NPs onto MOF is widely investigated as gas adsorbents[38–40] and catalysts used in hydrogenation[38,41–44] and cross coupling[42,45] reactions.[46] It can be noted that one of the most common approaches to obtain Pd^0@MOFs is using H$_2$ to reduce Pd^{2+}-precursor loading MOFs that are prepared *via* solution impregnation by soluble Pd^{2+} species. In some cases, trace amount of Pd^{2+} can be still observed after reduction.[45] Actually, according to the

^{a}Inorganic Chemistry II—Organometallics and Materials Chemistry, Ruhr-University Bochum, Universitätsstraße 150, 44801 Bochum, Germany
^{b}Institute of Chemical Technology, Universität Leipzig, Linnéstraße 3, 04103 Leipzig, Germany
^{c}Laboratory of Industrial Chemistry, Ruhr-University Bochum, Universitätsstraße 150, 44801 Bochum, Germany
^{d}Institute of Functional Interfaces (IFG), Karlsruhe Institute of Technology (KIT), 76344 Karlsruhe, Germany
^{e}Chair of Inorganic and Metal-Organic Chemistry, Department of Chemistry, Technical University Munich, Lichtenbergstraße 4, 85748 Garching, Germany
^{f}Catalysis Research Centre, Technical University Munich, Ernst-Otto-Fischer Strasse 1, 85748 Garching, Germany. E-mail: roland.fischer@tum.de
†Electronic supplementary information (ESI) available: Experimental details, IR, TGA, NMR, SEM-EDX, N$_2$ sorption, elementals analysis and catalytic reaction details. See DOI: 10.1039/c6dt02893d

concept of post-synthetic metal-ion exchange,[47] Pd^{2+} substitution in the metal nodes of MOFs could probably occur under this impregnation. Interestingly, the discrimination between the two Pd-sites (extra-framework loading or in-framework incorporation) is disregarded to some extent in the current literature. Given both facts, herein, an appropriate one-pot synthesis has been selected. Both H_2O and alcohols are found to be important components to reduce Pd^{2+} ions to Pd^0 at elevated temperatures.[48–50] Therefore, it is expected that utilizing a standard protocol for HKUST-1 synthesis (employing H_2O and EtOH under solvothermal conditions) can simultaneously introduce both Pd^{2+}-doped nodes and Pd^0 NPs in one step.

Pd@$[Cu_{3-x}Pd_x(BTC)_2]_n$ (**Cu/Pd-BTC_1–3**) materials have been synthesized under solvothermal conditions by mixing corresponding metal salts (Pd(II) acetate and $Cu(NO_3)_2\cdot3H_2O$) with H_3BTC directly in the starting reactions (see ESI†). All **Cu/Pd-BTC_1–3** samples (both as-synthesized and dried phases) are crystalline solids and isostructural with the parent Cu-BTC (Fig. 1 and S1†), indicating the preserved structure integrity after the Pd-sites introduction. Recorded PXRD patterns and accordingly calculated cell parameters of **Cu/Pd-BTC_1–3** match very well with the respective simulated data of the reported $[Cu_3(BTC)_2]_n$ single-crystal structure (Fig. S3 and Table S1†). Remarkably, intensity of the reflections at *ca.* 6.67°, 9.40° and 13.34° (2θ) assigned to the (200), (220) and (400) planes, respectively, varies (Fig. 1). This indicates certain changes of electronic density compared to the non-doped Cu-analogue (Cu-BTC). The main contribution to the reflection of the (200) and (220) planes is due to the metal-nodes (Fig. S4†). Hence, such difference in intensities should primarily stem from the partial substitution of Cu^{2+} by Pd^{2+} within the M_2-paddlewheel units of MOFs, indicating Pd^{2+} framework incorporation. Considering the presence of Pd NPs in the discussed **Cu/Pd-BTC_1–3**, small reflections at 40.02° resulting from (111) planes of the face-centered cubic structure of Pd are observed (Fig. 1).[51] This is probably due to the rather small particle size of these Pd NPs and therefore, they are difficult to be detected by PXRD technique. Finally, it should be pointed out that employing equal molar amounts of Cu- and Pd-salts

or only Pd-precursor in the starting reaction mixtures, formation of only metal/metal–oxide products has been observed (Fig. S5 and S6†).

AAS analysis of the activated **Cu/Pd-BTC_1–3** solids confirms quantitative incorporation of palladium. Thus, the Pd-contents and Pd : Cu ratios in the final **Cu/Pd-BTC_1–3** samples remain almost unchanged with respect to the taken feeding ratios of the metal-precursors (Table S2†). Furthermore, SEM-EDX elemental mapping demonstrates quite homogeneous Cu/Pd distribution within the obtained **Cu/Pd-BTC** solids (Fig. S8†). Incorporation of Pd^{2+} into the framework as well as the Pd^0 NPs loading has been subsequently corroborated by high-resolution XPS. Fig. 2 shows the Pd 3d core-level spectra of the **Cu/Pd-BTC_1** and **Cu/Pd-BTC_3** (representative samples with relatively low and high Pd-contents). Three Pd 3d doublets ($3d_{5/2}$ and $3d_{3/2}$) are resolved in the deconvoluted spectra. The doublet located at 337.9 and 343.2 eV (Pd2) is characteristic for Pd^{2+} species (Table S3†).[52,53] In addition, the higher binding energies observed at 338.9 and 344.2 eV for Pd1 reveal the presence of an electronically modified Pd^{2+} species. Moreover, we could unambiguously rule out an assignment of both Pd^{2+} species to PdO NPs, as no typical O 1s peak at about 530 eV has been detected in the corresponding spectra, which showed only one O 1s peak at 531.8 eV, originating from the carboxylate (–COO) groups in the frameworks. Therefore, both the found Pd^{2+} species (Pd1 and Pd2) are very likely associated with the formation of Pd–Pd and Cu–Pd framework-nodes. The doublet at *ca.* 335.8 and 341.0 eV is attributed to metallic Pd^0 species (Pd3), indicating the existence of Pd metallic NPs in these samples. Moreover, the amount of Pd NPs in the total Pd species (Pd^{2+} and Pd^0) increases (from 33% for **Cu/Pd-BTC_1** to 44% for **Cu/Pd-BTC_3**) along with the doping increase of Pd(II) acetate. TEM characterization has not been performed because of the beam sensitivity of HKUST-1, which does not allow characterization of the "pristine" Pd@$[Cu_{3-x}Pd_x(BTC)_2]_n$ sample as well.
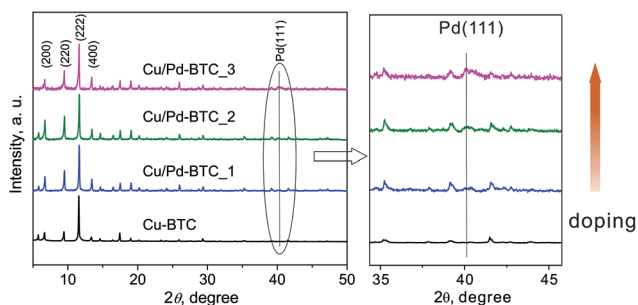

Fig. 1 PXRD patterns of activated Pd@$[Cu_{3-x}Pd_x(BTC)_2]_n$ (**Cu/Pd-BTC_1–3**) in comparison with activated non-doped Cu-BTC. The vertical lines correspond to the peak position of (111) planes of the face-centered cubic (fcc) Pd-structure.
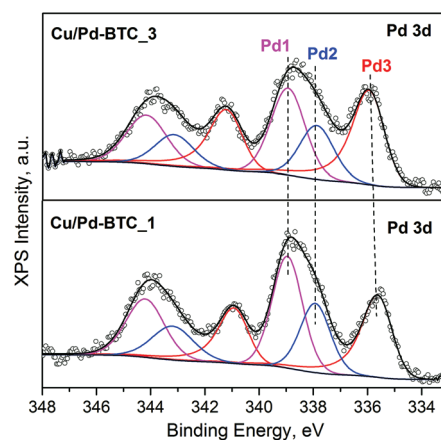

Fig. 2 Deconvoluted XP spectra of **Cu/Pd-BTC_1** and **3** in Pd 3d region.

Furthermore, any vibrations stemming neither from the non-reacted H_3BTC linker nor used metal-precursors (i.e., acetate-, nitrate-groups) could be revealed in the FT-IR spectra of all prepared **Cu/Pd-BTC** solids (Fig. S12†). Moreover, ^{1}H-NMR spectra of the digested **Cu/Pd-BTC_1–3** samples show the presence of only BTC-linker (Fig. S13†). Thus, absence of any resonances at about 1.9 ppm, stemming from the acetate protons, fully supports the IR results ruling out any residuals of the employed starting Pd-reactant. Hence, the presence of Pd^{2+}-sites should originate from the in-framework nodes rather than Pd^{2+}-precursor loading.

TGA suggests that thermal stability of the obtained **Cu/Pd-BTC_1–3** solids is fully preserved (in comparison with the parent **Cu-BTC**)[35] with the decomposition temperatures close to 300 °C (Fig. S14†). The N_2 (77 K) sorption isotherms recorded for obtained samples reveal type I isotherm (Fig. S15†), confirming their permanent microporosity. Brunauer–Emmett–Teller (BET) surface area of **Cu/Pd-BTC_1** and **_2** increase a little in comparison with the parent Cu-BTC (prepared under similar conditions) (Table S4†), indicating that the presence of Pd^{2+} incorporation as metal nodes in the framework are dominant. When it turns to **Cu/Pd-BTC_3**, the increasing of Pd^0 NPs results in a slight lower BET surface area in comparison with the others samples.

Both Pd^{2+}-containing MOF ($[Pd(2\text{-pymo})_2]_n$, 2-pymo = 2-pyrimidinolate)[31–33] and Pd^0@MOF,[38,42,43,45] have been reported as good reusable catalysts in typical palladium-catalyzed reactions such as Suzuki C–C couplings and hydrogenation. Owing to both Pd^0 NPs and potential Pd^{2+}-CUS (that should be available after thermal treatment and specifically promote H_2 splitting) in obtained Pd-containing Cu/Pd-BTC materials, it was of interest to test their catalytic activity in hydrogenation reactions. Herein, it should be mentioned that in order to investigate which Pd species (Pd^{2+} or Pd^0) would play the important role on the catalysis as well, we prepared another isostructural analog **Cu/Pd-BTC_4** sample employing $PdCl_2$ and longer reaction time instead (see ESI for the preparation and characterization: Tables S2, S3 and Fig. S2, S9, S11, S16†). This sample contains dominant Pd^0 (70%) rather than Pd^{2+} on the basis of the Pd 3d region XP spectra (Fig. S11 and Table S3†).

As a test reaction, the aqueous-phase hydrogenation of PNP to PAP using $NaBH_4$ as a reducing agent has been chosen. It can be conducted at room temperature and ambient pressure within a reaction time of <10 min using a simple on-line UV-Vis spectroscopy to monitor the progress of the reaction.[43,54,55] The concentration of PNP as a function of time as well as the initial reaction rate normalized to the amount of Pd in the catalyst for **Cu/Pd-BTC_1–4** are depicted in Fig. 3. Before addition of the solid catalyst, i.e., within the first 0.5 min of the experiment, no PNP conversion was observed. Complete conversion of PNP to PAP was reached within 2 min of reaction time using **Cu/Pd-BTC_1–4**, whereas the conversion of PNP remained incomplete for the Pd-free **Cu-BTC**. This incomplete conversion is known for catalysts with low activity and results from unproductive $NaBH_4$ decomposition to hydrogen.[54]
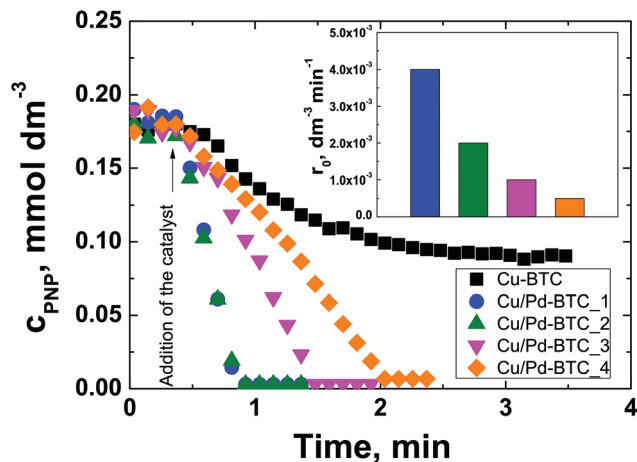

Fig. 3 Concentration of PNP as a function of time for non-doped Cu-BTC and Pd containing **Cu/Pd-BTC_1–4** as catalysts in the aqueous-phase hydrogenation of PNP with $NaBH_4$ to PAP. The insert shows the initial reaction rate for **Cu/Pd-BTC_1–4** normalized to the amount of Pd in the catalyst, respectively. Reaction conditions: c_{PNP} = 0.18 mmol dm^{-3}, c_{NaBH_4} = 0.60 mmol dm^{-3}, T = 298 K, stirring speed = 1300 min^{-1}, $m_{catalyst}$ = 5.0 mg, ambient pressure.

Evidently, the Pd-containing **Cu-BTC** catalysts are significantly more active than the Pd-free **Cu-BTC**. Interestingly, the initial reaction rate related to the Pd amount for **Cu/Pd-BTC_1** and **2** (i.e., 4.0×10^{-3} and 2.0×10^{-3} dm^{-3} min^{-1}) is significantly higher than that achieved over a metallic Pd catalyst supported on an Al-containing mesocellular silica foam (1.0×10^{-3} dm^{-3} min^{-1}) under the same reaction conditions.[56] Note that the activity of **Cu/Pd-BTC_1** and **2** is so high that the difference in their catalytic activity cannot be distinguished under the reaction conditions used.

Surprisingly, the normalized initial reaction rate decreases with increasing overall Pd content from 4×10^{-3} dm^{-3} min^{-1} for **Cu/Pd-BTC_1** to 1.0×10^{-3} dm^{-3} min^{-1} for **Cu/Pd-BTC_3**, respectively (insert in Fig. 3). This can be explained by considering the decreasing concentration of Pd^{2+} species with increasing Pd content from **Cu/Pd-BTC_1** to **Cu/Pd-BTC_3**, as observed by XPS (Table S3†). Particularly, **Cu/Pd-BTC_4** containing the lowest concentration of Pd^{2+} species (70%) displays the lowest initial reaction rate in comparison with the other three **Cu/Pd-BTC** samples. It may, therefore, be concluded that Pd^{2+} species in the catalyst are catalytically active and they are dominantly responsible for the observed high catalytic activity. Moreover, it has been reported that Pd^{2+} can act as active metal sites in olefin hydrogenations.[31–33] It can be noted that PXRD patterns of the **Cu/Pd-BTC** samples before and after reaction indicate that the structure of the framework remains unchanged (Fig. S17†). Finally, according to the ICP-OES analysis of the solution after reaction (**Cu/Pd-BTC_2** as selective catalysts), leaching of palladium is negligible (i.e., 0.01 mg L^{-1}), indicating the stability of the used MOF catalysts as well as the heterogeneous nature of the catalytic reaction.

In summary, *via* one-pot synthesis, we successfully obtained crystalline porous $Pd@[Cu_{3-x}Pd_x(BTC)_2]_n$ MOFs with various doping levels of Pd. On the basis of entire experimental data, structural incorporation of Pd^{2+} serving as frameworks-nodes (within Cu–Pd or/and Pd–Pd paddlewheels) as well as Pd^0 NPs dispersion in the framework of HKUST-1 are concluded. To the best of our knowledge, it is the singular case of MOFs bearing both Pd^{2+}-paddlewheels and Pd NPs known so far. Moreover, distinct Pd sites, especially Pd^{2+}/M-CUS considerably enhances the catalytic activity of MOFs in the aqueous-phase hydrogenation of PNP to PAP with respect to the "Pd-free" Cu-BTC catalysts, which affords a perspective way to tune their catalytic activity. Furthermore, a synthesis of HKUST-1 analogs excluding Pd^0 formation and featuring exclusive Pd^{2+}/Cu^{2+} mixed-metal paddlewheels would lead to highly active catalysts.

Notes and references

1 M. Latroche, S. Surblé, C. Serre, C. Mellot-Draznieks, P. L. Llewellyn, J.-H. Lee, J.-S. Chang, S. H. Jhung and G. Férey, *Angew. Chem., Int. Ed.*, 2006, **45**, 8227–8231.

2 K. Sumida, D. L. Rogow, J. A. Mason, T. M. McDonald, E. D. Bloch, Z. R. Herm, T.-H. Bae and J. R. Long, *Chem. Rev.*, 2012, **112**, 724–781.

3 E. D. Bloch, W. L. Queen, R. Krishna, J. M. Zadrozny, C. M. Brown and J. R. Long, *Science*, 2012, **335**, 1606–1610.

4 A. Corma, H. García and F. X. Llabrés i Xamena, *Chem. Rev.*, 2010, **110**, 4606–4655.

5 P. Horcajada, C. Serre, M. Vallet-Regí, M. Sebban, F. Taulelle and G. Férey, *Angew. Chem., Int. Ed.*, 2006, **45**, 5974–5978.

6 A. A. Talin, A. Centrone, A. C. Ford, M. E. Foster, V. Stavila, P. Haney, R. A. Kinney, V. Szalai, F. El Gabaly, H. P. Yoon, F. Léonard and M. D. Allendorf, *Science*, 2014, **343**, 66–69.

7 L. E. Kreno, K. Leong, O. K. Farha, M. Allendorf, R. P. Van Duyne and J. T. Hupp, *Chem. Rev.*, 2012, **112**, 1105–1125.

8 H. Deng, S. Grunder, K. E. Cordova, C. Valente, H. Furukawa, M. Hmadeh, F. Gándara, A. C. Whalley, Z. Liu, S. Asahina, H. Kazumori, M. O'Keeffe, O. Terasaki, J. F. Stoddart and O. M. Yaghi, *Science*, 2012, **336**, 1018–1023.

9 H. Deng, C. J. Doonan, H. Furukawa, R. B. Ferreira, J. Towne, C. B. Knobler, B. Wang and O. M. Yaghi, *Science*, 2010, **327**, 846–850.

10 A. Schneemann, V. Bon, I. Schwedler, I. Senkovska, S. Kaskel and R. A. Fischer, *Chem. Soc. Rev.*, 2014, **43**, 6062–6096.

11 D. Yan, G. O. Lloyd, A. Delori, W. Jones and X. Duan, *ChemPlusChem*, 2012, **77**, 1112–1118.

12 A. Carné-Sánchez, I. Imaz, M. Cano-Sarabia and D. Maspoch, *Nat. Chem.*, 2013, **5**, 203–211.

13 Z. Fang, B. Bueken, D. E. De Vos and R. A. Fischer, *Angew. Chem., Int. Ed.*, 2015, **54**, 7234–7254.

14 F. Vermoortele, B. Bueken, G. Le Bars, B. Van de Voorde, M. Vandichel, K. Houthoofd, A. Vimont, M. Daturi, M. Waroquier, V. Van Speybroeck, C. Kirschhock and D. E. De Vos, *J. Am. Chem. Soc.*, 2013, **135**, 11465–11468.

15 O. Kozachuk, I. Luz, F. X. Llabrés i Xamena, H. Noei, M. Kauer, H. B. Albada, E. D. Bloch, B. Marler, Y. Wang, M. Muhler and R. A. Fischer, *Angew. Chem., Int. Ed.*, 2014, **53**, 7058–7062.

16 C. K. Brozek and M. Dincă, *J. Am. Chem. Soc.*, 2013, **135**, 12886–12891.

17 G.-T. Vuong, M.-H. Pham and T.-O. Do, *Dalton Trans.*, 2013, **42**, 550–557.

18 D. F. Sava Gallis, M. V. Parkes, J. A. Greathouse, X. Zhang and T. M. Nenoff, *Chem. Mater.*, 2015, **27**, 2018–2025.

19 R. Shannon, *Acta Crystallogr., Sect. A: Cryst. Phys., Diffr., Theor. Gen. Cryst.*, 1976, **32**, 751–767.

20 O. Kozachuk, K. Khaletskaya, M. Halbherr, A. Bétard, M. Meilikhov, R. W. Seidel, B. Jee, A. Pöppl and R. A. Fischer, *Eur. J. Inorg. Chem.*, 2012, **2012**, 1688–1695.

21 Y. Jiao, C. R. Morelock, N. C. Burtch, W. P. Mounfield, J. T. Hungerford and K. S. Walton, *Ind. Eng. Chem. Res.*, 2015, **54**, 12408–12414.

22 F. Gul-E-Noor, B. Jee, M. Mendt, D. Himsl, A. Pöppl, M. Hartmann, J. Haase, H. Krautscheid and M. Bertmer, *J. Phys. Chem. C*, 2012, **116**, 20866–20873.

23 M. V. Parkes, D. F. Sava Gallis, J. A. Greathouse and T. M. Nenoff, *J. Phys. Chem. C*, 2015, **119**, 6556–6567.

24 M. A. Gotthardt, R. Schoch, S. Wolf, M. Bauer and W. Kleist, *Dalton Trans.*, 2015, **44**, 2052–2056.

25 Q. Zhang, L. Cao, B. Li and L. Chen, *Chem. Sci.*, 2012, **3**, 2708–2715.

26 N. Y. Kozitsyna, S. E. Nefedov, F. M. Dolgushin, N. V. Cherkashina, M. N. Vargaftik and I. I. Moiseev, *Inorg. Chim. Acta*, 2006, **359**, 2072–2086.

27 N. S. Akhmadullina, N. V. Cherkashina, N. Y. Kozitsyna, I. P. Stolarov, E. V. Perova, A. E. Gekhman, S. E. Nefedov, M. N. Vargaftik and I. I. Moiseev, *Inorg. Chim. Acta*, 2009, **362**, 1943–1951.

28 G. Nickerl, U. Stoeck, U. Burkhardt, I. Senkovska and S. Kaskel, *J. Mater. Chem. A*, 2014, **2**, 144–148.

29 J. M. Teo, C. J. Coghlan, J. D. Evans, E. Tsivion, M. Head-Gordon, C. J. Sumby and C. J. Doonan, *Chem. Commun.*, 2016, **52**, 276–279.

30 J. A. R. Navarro, E. Barea, J. M. Salas, N. Masciocchi, S. Galli, A. Sironi, C. O. Ania and J. B. Parra, *Inorg. Chem.*, 2006, **45**, 2397–2399.

31 F. X. Llabrés i Xamena, A. Abad, A. Corma and H. Garcia, *J. Catal.*, 2007, **250**, 294–298.

32 S. Schuster, E. Klemm and M. Bauer, *Chem. – Eur. J.*, 2012, **18**, 15831–15837.

33 S. Opelt, V. Krug, J. Sonntag, M. Hunger and E. Klemm, *Microporous Mesoporous Mater.*, 2012, **147**, 327–333.

34 X. Zhang, H. Xu, X. Liu, D. L. Phillips and C. Zhao, *Chem. – Eur. J.*, 2016, **22**, 7288–7297.

35 S. S. Y. Chui, S. M. F. Lo, J. P. H. Charmant, A. G. Orpen and I. D. Williams, *Science*, 1999, **283**, 1148–1150.

36 J. Szanyi, M. Daturi, G. Clet, D. R. Baer and C. H. F. Peden, *Phys. Chem. Chem. Phys.*, 2012, **14**, 4383–4390.

37 P. St. Petkov, G. N. Vayssilov, J. Liu, O. Shekhah, Y. Wang, C. Wöll and T. Heine, *ChemPhysChem*, 2012, **13**, 2025–2029.

38 M. Sabo, A. Henschel, H. Frode, E. Klemm and S. Kaskel, *J. Mater. Chem.*, 2007, **17**, 3827–3832.

39 C. Zlotea, R. Campesi, F. Cuevas, E. Leroy, P. Dibandjo, C. Volkringer, T. Loiseau, G. Férey and M. Latroche, *J. Am. Chem. Soc.*, 2010, **132**, 2991–2997.

40 G. Li, H. Kobayashi, J. M. Taylor, R. Ikeda, Y. Kubota, K. Kato, M. Takata, T. Yamamoto, S. Toh, S. Matsumura and H. Kitagawa, *Nat. Mater.*, 2014, **13**, 802–806.

41 S. Opelt, S. Türk, E. Dietzsch, A. Henschel, S. Kaskel and E. Klemm, *Catal. Commun.*, 2008, **9**, 1286–1290.

42 B. Gole, U. Sanyal, R. Banerjee and P. S. Mukherjee, *Inorg. Chem.*, 2016, **55**, 2345–2354.

43 C. Wang, H. Zhang, C. Feng, S. Gao, N. Shang and Z. Wang, *Catal. Commun.*, 2015, **72**, 29–32.

44 X. Jia, S. Wang and Y. Fan, *J. Catal.*, 2015, **327**, 54–57.

45 B. Yuan, Y. Pan, Y. Li, B. Yin and H. Jiang, *Angew. Chem., Int. Ed.*, 2010, **49**, 4054–4058.

46 M. Gulcan, M. Zahmakiran and S. Özkar, *Appl. Catal., B*, 2014, **147**, 394–401.

47 P. Deria, J. E. Mondloch, O. Karagiaridi, W. Bury, J. T. Hupp and O. K. Farha, *Chem. Soc. Rev.*, 2014, **43**, 5896–5912.

48 B. P. Fors, P. Krattiger, E. Strieter and S. L. Buchwald, *Org. Lett.*, 2008, **10**, 3505–3508.

49 T. A. Stephenson, S. M. Morehouse, A. R. Powell, J. P. Heffer and G. Wilkinson, *J. Chem. Soc.*, 1965, 3632–3640, DOI: 10.1039/JR9650003632.

50 W. A. Carole and T. J. Colacot, *Chem. – Eur. J.*, 2016, **22**, 7686–7695.

51 G. H. Jeong, S. H. Kim, M. Kim, D. Choi, J. H. Lee, J.-H. Kim and S.-W. Kim, *Chem. Commun.*, 2011, **47**, 12236–12238.

52 H.-F. Wang, W. E. Kaden, R. Dowler, M. Sterrer and H.-J. Freund, *Phys. Chem. Chem. Phys.*, 2012, **14**, 11525–11533.

53 R. Arrigo, M. E. Schuster, Z. Xie, Y. Yi, G. Wowsnick, L. L. Sun, K. E. Hermann, M. Friedrich, P. Kast, M. Hävecker, A. Knop-Gericke and R. Schlögl, *ACS Catal.*, 2015, **5**, 2740–2753.

54 M. Goepel, M. Al-Naji, P. With, G. Wagner, O. Oeckler, D. Enke and R. Gläser, *Chem. Eng. Technol.*, 2014, **37**, 551–554.

55 J. Sun, Y. Fu, G. He, X. Sun and X. Wang, *Catal. Sci. Technol.*, 2014, **4**, 1742–1748.

56 M. Al-Naji, A. M. Balu, A. Roibu, M. Goepel, W.-D. Einicke, R. Luque and R. Glaser, *Catal. Sci. Technol.*, 2015, **5**, 2085–2091.